Effects of fasting induced carbohydrate depletion on murine ischemic skeletal muscle function.

Cameron A. Schmidt[1,2], Emma J. Goldberg[1,2], Tom D. Green[1,2], Reema R. Karnekar[1,2], Jeffrey J. Brault[1,3], Spencer G. Miller[3], Adam J. Amorese[1,2], Dean J. Yamaguchi[4,5], Espen E. Spangenburg[1,2], Joseph M. McClung[1,2,4*]

[1]Dept. of Physiology, Brody School of Medicine, East Carolina University, Greenville, North Carolina, United States of America

[2]East Carolina Diabetes and Obesity Institute, East Carolina University, Greenville, North Carolina, United States of America

[3]Dept. of Kinesiology, College of Health and Human Performance, East Carolina University, Greenville, North Carolina, United States of America

[4]Department of Cardiovascular Sciences, East Carolina University, Greenville, North Carolina, United States of America

[5]Division of Surgery, Brody School of Medicine, East Carolina University, Greenville, North Carolina, United States of America

*Corresponding Author

Email: mcclungj@ecu.edu (J.M.M.)

Abstract

Stored muscle carbohydrate supply and energetic efficiency constrain muscle functional capacity during exercise and are influenced by common physiological variables (e.g. age, diet, and physical activity level). Whether these constraints affect overall functional capacity or the timing of muscle energetic failure during acute ischemia is not known. We interrogated skeletal muscle contractile properties in two anatomically distinct hindlimb muscles that have well characterized differences in energetic efficiency (locomotory- extensor digitorum longus (EDL) and postural- soleus muscles) under conditions of reduced carbohydrate supply**.** 180 mins of acute ischemia resulted in complete energetic failure in all muscles tested, indicated by: loss of force production, substantial reductions in total adenosine nucleotide pool intermediates, and increased adenosine nucleotide degradation product - inosine monophosphate (IMP). These changes occurred in the absence of apparent myofiber structural damage assessed histologically by both transverse section and whole mount. Restriction of the available intracellular carbohydrate pool by fasting (~50% decrease in skeletal muscle) did not significantly alter the timing to muscle functional impairment or affect the overall force/work capacities of either muscle type. Fasting did cause rapid development of passive tension in both muscle types, which may have implications for optimal timing of reperfusion or administration of precision therapeutics.

Introduction

Ischemic skeletal muscle necrosis occurs concurrently with several common clinical conditions (e.g. peripheral arterial disease, compartment syndrome, or diabetic necrosis) and is a complicating factor of successful muscle graft transplantation(1–3). The severity of necrosis during an ischemic episode has long been considered a sole function of time, temperature, and magnitude of the hypoxic insult(4,5). However, the timing of the events that precede irreversible functional impairment and necrosis during ischemia may also depend on other key variables including: metabolic rate; contractile efficiency; and the size of the stored carbohydrate pool(4). Carbohydrate metabolism is key, as muscle energy supply becomes dependent on anaerobic fermentation of stored carbohydrate sources during ischemia(6–8). Glycogen is the primary storage form of carbohydrate in skeletal muscle, and its storage/utilization can be influenced by acute environmental factors as well as chronic diseases(9–14).

Previous studies have examined the time dependent changes of metabolites and contractile function in rodent skeletal muscle following ischemia with reperfusion (I/R)(15–18). Several important observations can be gleaned from these studies: First, locomotory (fast glycolytic) muscles experienced more damage compared to postural (slow oxidative) muscles(15,17). Second, The degree of initial injury can have large effects on post ischemic recovery time(16). Lastly, Optimal reperfusion timing is related to changes in muscle metabolite levels during ischemia(18). A major limitation of I/R studies is that it is difficult to distinguish between the functional impairment and/or damage that is attributable to the ischemia itself versus that caused by the reperfusion injury.

In a previous study, using an *in vivo* mouse hindlimb ischemia model (without reperfusion), we found that myonecrosis develops between three and six hours after the onset of

ischemia and is accompanied by a complete loss of contractile function(19). This led us to examine the <3-hour time domain in this study to better characterize the exact temporal nature of muscle functional impairments and metabolite changes that occur under ischemic conditions. We hypothesized that reductions in stored muscle glycogen would significantly shorten the amount of time that the muscles could remain functional during ischemia. To test this hypothesis, we utilized fasting to induce an approximate 50% decrease in resting muscle glycogen and employed a carefully controlled experimental system to assess the effects of carbohydrate depletion on isolated mouse hindlimb muscle function during severe hypoxia and nutrient deprivation. Our data provide a novel characterization of ischemic muscle mechanical/energetic failure and paint a detailed picture of the timing of these impairments. This information will provide a valuable resource to be used in conjunction with studies of ischemia/reperfusion in mouse hindlimb ischemia models.

Materials and Methods

Animals

Adult male BALB/c mice (N=32), aged 16-24 weeks old, were obtained from Jackson Laboratories (Bar Harbor, ME). All work was approved by the Institutional Animal Care and Use Committee of East Carolina University. Animal care followed the Guide for the Care and Use of Laboratory Animals, Institute of Laboratory Animal Resources, Commission on Life Sciences, National Research Council. Washington: National Academy Press, 1996. Animals had free access to water and food except during fasting protocols, during which animals had free access to water only.

Laser scanning confocal and multiphoton microscopy

For microvascular imaging, Dylight 594 conjugated *Griffonia simplificolia* isolectin B_4 (GS-IB_4) (Vector Labs, Burlingame, CA) was injected retro-orbitally one hour prior to sacrifice. EDL and soleus muscles were dissected, and immersion fixed in 4% paraformaldehyde. BODIPY and DAPI staining was performed as previously described(20). Sarcomeric actin staining was performed in PFA fixed whole mount muscles, following permabilization with 30µg/ml saponin, using 200nM Alexa Fluor 488 conjugated phalloidin (Thermo Fisher, Waltham MA). For NAD(P)H autofluorescence imaging, live muscle was dissected following sacrifice and mounted at resting length. Live muscles were imaged in a glass bottom dish in Krebs Ringer solution. All imaging was performed using an Olympus FV1000 laser scanning confocal microscope (LSCM). Acquisition software was Olympus FluoView FSW (V4.2). The objective used was 60X oil immersion (NA=1.35, Olympus Plan Apochromat UPLSAPO60X(F)) or 30X (NA= 1.05, Olympus Plan Apochromat UPLSAPO30XS). Images were 800x800 pixel with 2µs/pixel dwell time. Detector noise was reduced by application of a 3X line scanning kalman filter. Images were acquired in sequential scan mode. 2µM DAPI was used for nuclear counterstaining (Sigma Aldrich, St. Louis, MO) and was excited using the 405nm line of a multiline argon laser; emission was filtered using a 490nm dichroic mirror and 430-470nm barrier filter. BODIPY and AF488-phalloidin were excited using the 488nm line of a multiline argon laser; emission was filtered using a 560nm dichroic mirror and 505-540nm barrier filter. Dylight 594 (GS-IB_4) was excited using a 559nm laser diode; emission was filtered using a 575-675nm barrier filter. Zero detector offset was used for all images. The pinhole aperture diameter was set to 105um (1 Airy disc). NAD(P)H autofluorescence has been shown to be highly localized to skeletal muscle mitochondria(21). NAD(P)H autofluorescence was excited using a mode locked pulsed laser (Mai Tai, Spectra Physics, Santa Clara, CA) tuned to 720nm. Emission was collected using separate non-descanned detectors.

Dystrophin/Laminin immunofluorescence in transverse muscle sections

EDL and soleus muscles were embedded in optimal cutting temperature medium (OCT), and frozen in liquid nitrogen cooled isopentane for cryosectioning. 10µm sections were cut using a CM-3050S cryostat (Leica, Wetzlar Germany) and collected on charged glass slides. Sections were then fixed in 1:1 acetone/methanol for 10 minutes at -20°C, rehydrated in 1X phosphate buffered saline (PBS), and blocked in 5% goat serum + 1X PBS for one hour at room temperature. Sections were then incubated with mouse anti-human monoclonal dystrophin antibody (Thermo-Fisher, MA5-13526), and rabbit anti-rat primary laminin antibody (Thermo-Fisher, A5-16287) at 4°C overnight. Sections were washed 3X for 10 minutes with cold 1X PBS and incubated for 1 hour with Alexa-fluor 594 conjugated goat anti-rabbit IgG or Alexa-fluor 488 conjugated goat anti-mouse (highly cross adsorbed) IgG2b secondary antibody (1:250, Invitrogen). Sections were mounted using Vectashield hard mount medium without Dapi (Vector Labs). Images were taken with an Evos FL auto microscope (Thermo Fisher, Waltham, MA) with a plan fluorite 20X cover slip corrected objective lens (NA = 0.5, air). The following excitation/emission filter cubes were used: GFP (470/22 nm Excitation; 510/42 nm Emission) and Texas Red (585/29 nm Excitation; 624/40 nm Emission). 4X and 20X magnification images were taken for each condition. Image processing was performed using ImageJ (NIH, v1.51f)(22).

Fasting

Pilot testing was performed to determine the minimal fasting time to achieve an ~50% reduction in resting skeletal muscle glycogen(23). Muscle glycogen reached the target reduction after 24 hours of fasting (one dark cycle).

Measurement of muscle mechanical function

Mice were sacrificed by cervical dislocation under isoflurane anesthesia (confirmed by lack of pedal withdrawal reflex). Extensor digitorum longus (EDL) or soleus muscles were carefully dissected and tied at both tendon ends with 5-0 silk sutures (Thermo Fisher, Waltham, MA). Muscles were tied to an anchor at the proximal end and a dual mode force transducer (Aurora 300B-LR, Aurora, ON, Canada) at the distal end in a vertical bath at 22°C. All protocols were performed in the absence of additional carbon fuel sources (i.e. amino acids, glucose, etc.) to restrict muscles to stored fuel supplies. The bath solution was a modified Krebs Ringer solution described previously(24). All muscles were dissected and mounted within 15 mins of sacrifice. Muscles were equilibrated in the bath for 10 mins, and optimal length (L_0) was determined by stimulating twitch contractions (0.2ms pulse width, 1 pulse/train) at 10 second intervals and adjusting the length incrementally until maximal force was achieved. Supramaximal stimulation voltage for both muscle types was determined to be 20V. L_O (mm) was measured using a digital microcaliper (Thermo Fisher, Waltham, MA). A force frequency curve was developed for each muscle using stepwise increasing stimulation frequencies of 10, 20, 40, 60, 80, 100, and 120 Hz (.2ms pulse width, pulses/train=half of the stim. Freq.). Baths were aerated with 95%O_2/5%CO_2 (oxygenated; O_2 condition) during L_O determination and the initial force frequency curve. The aeration source was then either left the same or changed to 95%N_2/5%CO_2 (hypoxic; N_2 condition) to simulate ischemia. The muscles were then equilibrated for 10 mins, and an initial isokinetic contraction protocol was elicited in the O_2 condition (100Hz isometric contraction for 0.8 seconds followed by a 3mm shortening phase over .3 seconds, then a return to L_o over 30s for the EDL; for the soleus 80Hz isometric contraction was elicited for 0.8 seconds followed by a 4mm shortening phase over .4 seconds, then a return to L_o over 30s). The aeration source was then either left the same or changed to 95%N_2/5%CO_2 (hypoxic condition), with experimental conditions alternated each time to reduce bias. The muscles were then equilibrated for 10 mins,

followed by stimulated isokinetic contractions every 10 mins for 180 mins (18 total contractions). We chose this timing based on our previous observation that excitation contraction coupling is impaired in muscles isolated from BALB/c mice 180 minutes after induction of acute hindlimb ischemia (in the absence of histological signs of tissue necrosis)(19). A second force frequency curve was measured following the 180-min. isokinetic protocol without changing the aeration source. Muscles were removed from the apparatus, blot dried on paper, weighed, and flash frozen in liquid nitrogen for biochemical analyses. Isometric time-tension integrals (TTI) were calculated by integrating over the isometric (phase I) portion of the curve and are expressed in units of $N*s/cm^2$. Isokinetic work (W) was obtained by integrating the force over the length change during the shortening (phase II) portion of the protocol and is expressed in units of J/cm^2.

Absolute isometric force measurements were normalized to mathematically approximated cross-sectional areas of the muscles. The cross-sectional area for each muscle was determined by dividing the mass of the muscle (g) by the product of its optimal fiber length (L_f, cm) and estimated muscle density (1.06 g cm^{-3}). Muscle force production was expressed as specific force (N/cm^2) determined by dividing the tension (N) by the calculated muscle cross-sectional area. L_f was obtained by multiplying L_O by the standard muscle length to fiber length ratio (0.45 for adult mouse EDL; 0.71 for soleus)(25). A gas calibrated Clark electrode (Innovative instruments, Lake Park, NC) was used to assess the oxygen saturation of the isolated bath medium under both aeration conditions prior to carrying out the experiments. O_2 conditions were approximately 90% saturation measured at the center of the bath (after 10 mins of aeration). N_2 conditions were <2% saturation.

Measurement of glycogen content in whole tissue

Skeletal muscle and liver tissues were flash frozen in liquid nitrogen and stored at -80°C. Glycogen assays were performed using acid hydrolysis and an enzyme coupled assay(26). Briefly, tissue samples were digested/hydrolyzed under acidic conditions using 2N hydrochloric acid (Sigma Aldrich, St. Louis, MO) on a heating block at 95°C for 2 hours with additional vortexing. Samples were neutralized with equal volume 2N sodium hydroxide (Sigma). A small amount of tris HCl pH 7.0 (~1% of final volume) was added to buffer the solution. Samples were added to a clear 96 well plate in duplicate and were incubated with a solution containing: >2000U/L hexokinase (S. *cerevisiae*), >4000 U/L NAD^+ dependent glucose-6-phosphate dehydrogenase (L. *mesenteroides*), 4mM ATP, 2mM Mg^{2+}, and 2mM NAD^+ (Hexokinase reagent solution; Thermo Fisher). Water was used in place of the reagent for background correction. A standard curve of D-glucose (Sigma Aldrich) was used to calculate the concentrations of hydrolyzed glucosyl units in each sample. Colorimetric measurement of NAD(P)H absorbance was made at 340nm using a Cytation 5 microtiter plate reader (Biotek, Winooski, VT). Liver samples were diluted 1:50 in water prior to enzyme coupled assays to obtain absorbance values within the range of the standard curve. Data were normalized to tissue mass and represented as nmoles glucose/mg tissue wet weight. The response coefficient (R_{Glyc}) is defined as the fractional change in experimental group mean relative to the basal group (i.e. Mean Basal – Mean Experimental/Mean Basal*100).

Ultra-performance liquid chromatography (UPLC) measurements of adenosine nucleotides in whole tissue

UPLC measurements of adenosine nucleotides in whole muscle tissue have been described in detail previously(27). Briefly, isolated muscles were flash frozen in liquid nitrogen, homogenized in ice-cold perchloric acid using a glass on glass homogenizer, and centrifuged to remove precipitated proteins. Samples were neutralized using

potassium hydroxide and centrifuged a second time, to remove perchlorate salt. Adenosine nucleotides and degradation products were assayed using an Acquity UPLC H class system (Waters, Milford, MA). Metabolites were identified by comparison of peak retention times of pure, commercially available standards (Sigma–Aldrich). These UPLC measures can provide an index of intracellular energetic state. The amount of IMP reflects longer periods of metabolic demand exceeding supply as the available adenylate pool is decreased via irreversible deamination of AMP to IMP. Over the timeframe of these stimulation protocols, IMP accumulation is a reliable measure of sustained mismatch between ATP supply and demand. (Adenosine triphosphate-ATP, adenosine diphosphate-ADP, adenosine monophosphate-AMP, and inosine monophosphate-IMP).

Statistical Analysis

Results of statistical comparisons are represented by means ± standard error (SEM). Sample variance (in figure panels) is represented by sample standard deviation (SD). Analyses and plotting were carried out using Graphpad prism (V8.01; Windows 10). Unpaired two-tailed t-tests were used for between group comparisons. For comparison of means, p values of < 0.05 were considered statistically significant.

Results

Extensor digitorum longus (EDL) and soleus muscles were chosen for their known differences in thermodynamic efficiency(28). The muscles also characteristically rely on different modes of energy metabolism (glycolytic and oxidative metabolism respectively)(29). The specialized nature of each muscle is highlighted for illustrative purposes by whole mount imaging (**Fig 1**), contrasting the dramatically different microvascular anatomy, cellular lipid droplet distribution (BODIPY), and mitochondrial density/distribution (NAD(P)H).

Fig 1: Microanatomy of Extensor digitorum longus (EDL) and soleus muscles differs in several key ways. Qualitative images highlighting a few of the key anatomical differences between the fast twitch extensor digitorum longus (EDL) and slow twitch soleus muscles (A). From left to right: (Left) Vessel density images are z-projections of Dylight 594 conjugated lectin; (Middle) BODIPY images are z-projections of BODIPY positive lipid droplets. Red signal in BODIPY images are lectin stained blood vessels. Blue signal in BODIPY images are myonuclei. Arrows indicate BODIPY positive lipid droplets in zoomed image inlays; (Right) Mitochondrial NAD(P)H images are optical sections of reduced pyridine nucleotide autofluorescence in live isolated skeletal muscle. NAD(P)H fluorescence intensity is mapped onto the image (highest intensity in white). Scale bars are 25um.

Fasting is a well characterized and effective method of whole body carbohydrate depletion in mice, due to their high thermal conductivity and large surface area to body volume ratio(23). This method was chosen for this study because it is independent of the confounding effects of exercise or contraction induced fatigue(30). The mean change in bodyweight over the fasted period (24 hours) was 3.9 ± 0.12 grams, approximately 13% of the mean initial weight. We observed a large difference in stored glycogen levels between fed and fasted groups in both liver (~90% lower) (**Table 1**) and skeletal muscle (~50% lower) (**Table 1**). Interestingly, the resting glycogen concentration was higher in the soleus than the EDL under both fed and fasted conditions. Additionally, soleus muscles had a lower mean glycogen concentration in the fasted group relative to the fed state (mean percent difference of 41.6% compared to 56.1% in the EDL groups; **Table 1**).

Table 1: Basal tissue glycogen concentrations in the liver and skeletal muscle of fed Vs. fasted groups.

Tissue	Condition	Glycogen (nmol/mg)	StDev (nmol/mg)	% Fed Group
Liver	Fed	387.9*	88.43	
	Fasted	42.0*	20.7	10.8
EDL	Fed	34.4*#	8.0	
	Fasted	19.3*#	3.2	56.1
Soleus	Fed	61.9*#	17.5	
	Fasted	25.8*#	3.6	41.6

Units are nanomoles hydrolyzed glucosyl units/milligram tissue wet weight (nmol/mg). *p<.05 Fed V. Fasted Groups. #p<.05 EDL V. Sol. N=4. Sample standard deviation (StDev).

Fasting had no effect on the isometric force-frequency relationship at baseline or under any of the tested conditions in the EDL (**Fig 2A**) or soleus (**Fig 2B**), indicating reduced carbohydrate pool size did not alter excitation-contraction coupling. Specific force values for both muscles were consistent with those obtained previously(24). Additionally, we observed characteristic reductions in maximal specific force following the O_2 protocols (and completely impaired force production following the N_2 protocols) in both muscles (**Fig 2A,B**). Notably, the isometric force capacity during each protocol did not differ between the fed and fasted groups in either the EDL (**Fig 2C**) or the soleus (**Fig 2D**). Similarly, the work capacity over the course of the protocols did not differ for either muscle between the fed and fasted states (**Fig 2E,F**). As expected, the force and work capacities were greatly reduced under the N_2 conditions compared to O_2 conditions.

Fig 2: Effects of carbohydrate depletion on excitation-contraction coupling and force/work capacities. Specific force-frequency curves for EDL (A) and soleus (B). Basal conditions are 95% O_2 prior to isokinetic protocol. (C,D) Specific force capacities were obtained by summing the isometric portion of the time-tension integrals at each sampling interval for the EDL and soleus respectively. (E,F) Specific work capacities were obtained by summing the isovelocity (shortening) portion of the length-tension integrals at each sampling interval for the EDL and soleus. N=8/treatment/group. Data are presented as mean ± SD. *p<.05 O_2 Vs. N_2 (Vs. Basal A,B).

Given that no substantial differences in force or work capacities were observed, we next examined whether the timing of muscle functional impairments would differ between the fed and fasted states. The time-tension integral (TTI) of the isometric portion of each contraction was plotted as a function of the number of contractions (or time) during each protocol for the EDL (**Fig 3A**) and soleus (**Fig 3B**). This measurement represents the ability of the muscle to perform sustained non-shortening contractions. Additionally, the length-time integral of the isokinetic portion of each contraction was also plotted against the number of contractions for the EDL (**Fig 3C**) and soleus (**Fig 3D**). This measurement represents the ability of the muscle to perform shortening work. Both sets of curves were characterized by an inverse linear relationship under O_2 conditions and a distinctly non-linear inverse relationship under N_2 conditions during the time and frequency domains of the experiments. The muscles from the fasted group experienced more rapid reduction in both TTI and work. All the tested muscles, however, experienced full impairment (defined as force or work output <10% of the initial value) within a relatively small (~10-20 min.) window of time. Passive tension was measured at the start of each contraction for the EDL (**Fig 3E**) and soleus (**Fig 3F**). This measurement represents stiffening of the muscle, which

may be due to several possible factors, including impaired calcium reuptake or cellular swelling due to uncontrolled fluid uptake(31). None of the muscles experienced substantial changes in passive tension during the O_2 protocol. Large increases in passive tension occurred in both muscles under N_2 conditions. Interestingly, passive tension development occurred earlier in the fasted groups (**Fig 3E,F**). To account for the possibility that the muscles were accumulating excessive water, the wet weights of the EDL (**Fig 3G**) and soleus (**Fig 3H**) were plotted. No differences in wet weight between the fed and fasted states were observed in either muscle, and all the tested muscles accumulated additional weight following the N_2 protocol.

Fig 3: Effects of carbohydrate depletion on the timing of functional impairment during ischemia. Isometric time-tension integrals (TTI) of each contraction over the course of 18 contractions (or 180 minutes) under each condition for the EDL (A) and soleus (B). Isokinetic length-tension integrals (isokinetic work) of each contraction for the EDL (C) and soleus (D). Developed passive tension (measured at the start of each contraction) for the EDL (E) and soleus (F). Muscle wet weights obtained at the end of each protocol for the EDL (G) and soleus (H). N=8/treatment/group. Data are presented as mean ± SD.

We next measured the muscle glycogen levels following the O_2 and N_2 protocols. The N_2 protocol reduced glycogen concentrations in all the muscles tested, relative to the O_2 condition (**Table 2**). Additionally, glycogen concentrations were lower in the fasted soleus groups compared to the fed groups under both O_2 and N_2 conditions (**Table 2**). However, glycogen concentrations did not differ between fed and fasted groups in the EDL muscles. Using the response coefficient (R_{Glyc}), allowed for comparison of each group mean to the

349 basal values that are presented in **Table 1**. The patterns among both muscle types were
350 similar when represented this way. The largest differences observed were between O_2
351 and N_2 conditions and were not substantially different between fed and fasted groups.
352 Interestingly, the smallest difference in glycogen concentration observed was in the fasted
353 O_2 condition for each muscle. This observation indicates the use of alternative (oxygen
354 dependent) fuel sources.

355

356 **Table 2: Tissue glycogen concentrations in EDL and soleus muscles of fed V. fasted mice**
357 **following O2 or N2 protocols.**

Tissue	Group	Condition	Glycogen(nmol/mg)	StDev(nmol/mg)	R_{Glyc} (%)
EDL	Fed	O_2	22.4†	4.4	-34.8
		N_2	7.9†	5.1	-77.0
	Fasted	O_2	18.8†	7.3	-2.5
		N_2	7.6†	1.3	-60.6
Soleus	Fed	O_2	42.1†*	6.6	-31.9
		N_2	29.0†*	1.6	-53.1
	Fasted	O_2	23.5†*	8.8	-8.9
		N_2	9.8†*	4.2	-62.0

358 Units are nanomoles hydrolyzed glucosyl units/milligram tissue wet weight (nmol/mg). The
359 Response Coefficient (R_{Glyc}¬) indicates the percent change relative to the baseline group means

(Presented in Table 1). Sample standard deviation (StDev). *p<.05 Fed V. Fasted Groups. †p<.05 O2 V. N2 Groups. N=4.

Total adenosine nucleotide (TAN) concentrations were examined as a measure of the aggregate tissue energetic state at the end of each protocol. Reductions in the concentrations of the total adenosine nucleotide pool, and accumulation of IMP, are measures of the muscles' inability to resynthesize ATP(27). Following the O_2 protocol, the TAN pool decreased slightly in both EDL (**Fig 4C**) and soleus (**Fig 4D**) muscles compared to our reported baseline values (**Fig 4 A,B**), but did not differ between fed and fasted groups. Following N_2 protocols, there were large decreases in the TAN pool in both the EDL (**Fig 4E**) and soleus (**Fig 4F**), with accompanying increases in the tissue IMP concentrations (**Fig 4G,H**). However, no substantial differences were observed between the fed and fasted groups for either muscle type.

Fig 4: Metabolic characteristics of isolated EDL and soleus muscles under limiting conditions of resting glycogen and oxygen availability. Total adenosine nucleotide concentrations at baseline for the EDL (A) and soleus (B). TAN concentrations following the 180 min. protocol in 95% O_2 for the EDL (C) and soleus (D). TAN concentrations following the 180 min. protocol in 95% N_2 (E,F). IMP accumulation after each protocol, compared across all three conditions for the EDL (G) and soleus (H). N=4/treatment/group. Data are presented as mean ± SD. *p≤.05 O2 V. N2 (V. Basal) Groups.

Previous reports have indicated that dystrophin IF staining is rapidly reduced in skeletal and cardiac muscle during early myonecrosis(19,32). Immunofluorescent staining for the

sarcolemmal protein dystrophin and the extracellular matrix protein laminin was performed on a subset of transverse sectioned muscles to assess the possibility that muscles were incurring damage during the contraction protocols. No apparent changes were observed in the EDL (**Fig 5A**) or soleus (**Fig 5C**) under O_2 or N_2 conditions, indicating that the muscle tissue remained intact during the experiments. Degradation of myofibrillar structures are another well characterized indicator of myonecrosis development(33). Parallel assessments were made to accompany the dystrophin/laminin stain. Fibrous actin was stained in fixed whole mount muscle specimens utilizing optical sectioning to assess the intramyofibrillar-IMF and perinuclear-PN regions of the myofibers at baseline and following the N_2 protocol in the EDL (**Fig 5B**) and soleus (**Fig 5D**). Together these assessments did not reveal any qualitative indication of damage.

Fig 5: Assessment of structural integrity of the muscles following experimental protocols. To control for the possibility that the muscles were structurally damaged during the contraction protocols, we performed immunofluorescence against sarcolemmal and extracellular matrix proteins. Image panels of dystrophin (green), and laminin (red) stained transverse EDL (A) and soleus (C) muscle sections under each of the conditions tested. Sarcomeric actin was stained using phalloidin (Cyan) in fixed/permeabilized whole mount muscles at baseline or following 180 mins of severe hypoxia (95% N_2); EDL (B) and soleus (D). Optical sectioning facilitated imaging in the intra-myofibrillar (IMF) and perinuclear (PN) regions of the muscle fibers. Scale bars are 1000μm (A, B Left Panel), 200 μm (A,B right panels), and 25 μm (B,D).

Discussion

Skeletal muscle is among the most metabolically dynamic tissues in the body, and is capable of sustaining a 100-fold change in ATP utilization rate during contraction(34). The total cost of ATP during contraction is proportional to the duration, intensity, and type (i.e. shortening vs. non-shortening)(35). Glycogen is the primary storage form of glucose in skeletal muscle, and is a major source of fuel during most forms of muscle activity(36). Importantly, glycogen is also the primary source of stored fuel utilized to regenerate ATP via substrate level phosphorylation in anaerobic glycolysis during severe hypoxia(35). Depletion of stored muscle glycogen by fasting or exhaustive exercise results in impaired fatigue resistance and recovery in isolated rodent muscles under normoxic conditions(36–38). Under ischemic conditions, this effect would be expected to lead to cumulative reductions in energetic capacity due to the inability to resynthesize ATP and phospho-creatine (PCr) that is used in support of contraction or resting metabolic processes. Overnight fasting in rodents results in more dramatic metabolic effects than human overnight fasting, but induces experimentally reproduceable reductions in systemic carbohydrate stores that are similar to more extreme physiological conditions such as hyperinsulinemia, hypoglycemia, or post exercise recovery(11,14,23,39). We were somewhat surprised to find that dramatically reduced muscle glycogen levels had no substantial effect on the timing or magnitude of muscle functional impairment under ischemic conditions. Our findings indicate that both muscle types retain a large pool of stored glycogen that is non-essential for reserve mechanical force production during hypoxia. It is not clear what the reserve glycogen pool contributes to *in vivo* during fasting. Future studies could be directed to investigate its' potential involvement in the maintenance of systemic glucose homeostasis through the production of free amino acids (i.e. alanine and glutamine) or lactate which can be converted to glucose in the liver(40,41).

In mouse EDL and soleus muscles, as much as 50% of the resting metabolic rate has been attributed to maintenance of intracellular calcium homeostasis(42). We observed a rapid increase in passive tension development in the fasted group relative to the fed group under N_2 conditions in both muscle types. The observed increase in the rate of passive tension development was the only measurement that was substantially different between the fed and fasted groups. This phenomenon is most likely indicative of progressive impairment of calcium handling as the capacity for ATP re-synthesis was gradually depleted(27). This effect may have implications for reperfusion timing, as it has been noted that calcium handling impairment prior to reperfusion is associated with poor salvage outcomes(4,43).

The dynamic requirements of ATP during muscle contraction require a similarly dynamic supply of carbon fuel sources that are derived from both blood and intracellular stores. Physiological and anatomical adaptations (i.e. capillary density, size of stored energy substrate pools, and mitochondrial density/function) are known to facilitate large differences in capacity for spontaneous vs. sustained exercise in different species(44). Similar adaptive differences are highlighted in the distinct microanatomical differences of mouse locomotory EDL and postural soleus muscles. These adaptive differences, combined with their similar size and relatively homogeneous fiber type compositions, make these muscles excellent candidates for comparative studies of muscle energy metabolism.

Skeletal muscle fiber types are categorized by a range of intrinsic metabolic and mechanical properties(45). Human muscles are generally of mixed fiber type, but mouse muscles consist of more homogeneous fiber type distributions, making them a practical model for studying fiber type specific effects (soleus: 1:1 slow type I/fast type IIa; EDL: 9:1 fast type IIb/fast type IIa)(29,46). At face value, it may seem intuitive that fast glycolytic

fiber types would be better suited to performance during hypoxia due to their preference for stored carbohydrate dependent energy metabolism(36,37,47). However, several studies have indicated a high degree of sensitivity of fast glycolytic muscles to ischemia/reperfusion injury(16,17,48). One important contributing factor to this effect is an energetic inefficiency of contraction due to interactions at the level of the acto-myosin crossbridges(28,49). In the present study, we observed that Soleus muscles stored more glycogen at baseline, had greater specific force/work capacities, and produced absolute force for a longer period during ischemia compared to EDL muscles. These observations are consistent with previous reports(48,50). Though the absolute differences in glycogen concentrations between groups were larger in the soleus compared to the EDL, the response coefficient (R_{Glyc}) which facilitates interpretation of group differences relative to their baseline concentration, indicated that the patterns of utilization were not different between the two types of muscles. We interpret these findings to mean that the greater basal glycogen concentration observed in the soleus muscles was likely not the primary factor underlying it's enhanced ischemic mechanical performance.

Conclusion

Investigating the key factors that affect the timing of muscle energetic failure during ischemia will aid in identifying optimal windows for therapeutic intervention. We predicted that the amount of stored carbohydrate is one such factor, as it is a major contributor to anaerobic energy metabolism and is influenced by several physiologically relevant conditions. We conclude that mouse hindlimb muscles maintain a large pool of stored carbohydrate that is utilized during fasting but does not contribute substantially to the timing of functional decline during acute ischemia. The carbohydrate lowering effects of fasting did not substantially affect the total capacity or timing of contractile function impairment in either muscle type. However, fasting did result in substantial increases in

early passive tension development, which may have implications for the timing of reperfusion or therapeutic administration. We also found that soleus muscles maintained a greater total force capacity and became impaired more slowly than EDL muscles, independent of glycogen utilization during the experimental period. This finding supports several previous observations and bolsters the notion that susceptibility to acute ischemic injury is not uniform across muscle types.

References:

1. Liu J, Saul D, Böker KO, Ernst J, Lehman W, Schilling AF. Current Methods for Skeletal Muscle Tissue Repair and Regeneration. Biomed Res Int. 2018;2018:1–11.
2. Dolan NC, Liu K, Criqui Michael H, Greenland P, Guralnik Jack M, Chan C, et al. Peripheral artery disease, diabetes, and reduced lower extremity functioning. Diabetes Care. 2002;25(1):113–20.
3. Callum K, Bradbury A. ABC of arterial and venous disease: Acute limb ischaemia. BMJ. 2000;320(7237):764–7.
4. Paradis S, Charles A-L, Meyer A, Lejay A, Scholey JW, Chakfé N, et al. Chronology of mitochondrial and cellular events during skeletal muscle ischemia-reperfusion. Am J Physiol - Cell Physiol. 2016;310(11):C968–82.
5. Petrasek PF, Homer-Vanniasinkam S, Walker PM. Determinants of ischemic injury to skeletal muscle. J Vasc Surg. 1994;19(4):623–31.
6. Jansson E, Johansson J, Sylven C, Kaijser L. Calf muscle adaptation in intermittent claudication. Side-differences in muscle metabolic characteristics in patients with unilateral arterial disease. Clin Physiol. 1988;8(1):17–29.
7. Theodore Kalogeris, Christopher P. Baines, Maike Krenz RJK. Cell Biology of Ischemia/Reperfusion Injury. Int Rev Cell Mol Biol. 2012;298:229–317.

8. Spriet LL, Soderlund K, Bergstrom M, Hultman E. Anaerobic energy release in skeletal muscle during electrical stimulation in men. J Appl Physiol. 1987;62(2):611–5.

9. Damsbo P, Vaag A, Hother-Nielsen O, Beck-Nielsen H. Reduced glycogen synthase activity in skeletal muscle from obese patients with and without Type 2 (non-insulin-dependent) diabetes mellitus. Diabetologia. 1991;34(4):239–45.

10. Bergstrom J, Hermansen L, Hultman E, Saltin B. Diet, Muscle Glycogen and Physical Performance. Acta Physiol Scandanavia. 1967;(71):140–50.

11. Vollestad NK, Blom C. Effect of varying intensity on glyocgen depletion in human muscle fibres. Acta Physiol Scand. 1985;125:395–405.

12. Askew CD, Green S, Walker PJ, Kerr GK, Green AA, Williams AD, et al. Skeletal muscle phenotype is associated with exercise tolerance in patients with peripheral arterial disease. J Vasc Surg. 2005;41(5):802–7.

13. McGuigan MR, Bronks R, Newton RU, Sharman MJ, Graham JC, Cody D V, et al. Muscle fiber characteristics in patients with peripheral arterial disease. Med Sci Sports Exerc. 2001;33(12):2016–21.

14. Cohen N, Rossetti L, Shlimovich P, Halberstam M, Hu M, Shamoon H. Counterregulation of hypoglycemia: Skeletal muscle glycogen metabolism during three hours of physiological hyperinsulinemia in humans. Diabetes. 1995;44(4):423–30.

15. Woitaske MD, McCarter RJ. Effects of fiber type on ischemia-reperfusion injury in mouse skeletal muscle. Vol. 102, Plastic and reconstructive surgery. 1998. p. 2052–63.

16. Vignaud A, Hourde C, Medja F, Agbulut O, Butler-Browne G, Ferry A. Impaired skeletal muscle repair after ischemia-reperfusion injury in mice. J Biomed Biotechnol. 2010;2010.

17. Chan RK, Austen WG, Ibrahim S, Ding GY, Verna N, Hechtman HB, et al. Reperfusion injury to skeletal muscle affects primarily type II muscle fibers. J Surg Res. 2004;122(1):54–60.

18. Idstrom J, Soussi B, Elander A, Bylund-Fellenius A. Purine metabolism after in vivo ischemia and reperfusion in rat skeletal muscle. Am Physiol Soc. 1990;258(6):1668–73.

19. Schmidt CA, Amorese AJ, Ryan TE, Goldberg EJ, Tarpey MD, Green TD, et al. Strain-Dependent Variation in Acute Ischemic Muscle Injury. Am J Pathol. 2018 May 1;188(5):1246–62.

20. Spangenburg EE, Pratt SJP, Wohlers LM, Lovering RM. Use of BODIPY (493/503) to visualize intramuscular lipid droplets in skeletal muscle. J Biomed Biotechnol. 2011;

21. Rothstein EC, Carroll S, Combs CA, Jobsis PD, Balaban RS. Skeletal muscle NAD(P)H two-photon fluorescence microscopy in vivo: Topology and optical inner filters. Biophys J. 2005;88(3):2165–76.

22. Schneider CA, Rasband WS, Eliceiri KW. NIH Image to ImageJ: 25 years of image analysis. Nat Methods. 2012 Jun;9(7):671–5.

23. Jensen TL, Kiersgaard MK, Sørensen DB, Mikkelsen LF. Fasting of mice: A review. Lab Anim. 2013;47(4):225–40.

24. Tarpey MD, Amorese AJ, Balestrieri NP, Ryan TE, Schmidt CA, McClung JM, et al. Characterization and utilization of the flexor digitorum brevis for assessing skeletal muscle function. Skelet Muscle. 2018;8(1):1–15.

25. Barton ER, Lynch G, Khurana TS, Grange RW, Raymackers J-M, Dorchies O, et al. Measuring isometric force of isolated mouse muscles in vitro. Exp Protoc DMD Anim Model Treat-NMD Neuromuscul Network. 2008;1(2):14.

26. Passonneau J V, Lauderdale VR. A Comparison of Three Methods of Glycogen

565 Measurement in Tissues. Anal Biochem. 1974;60(2):405–12.
566 27. Brault JJ, Pizzimenti NM, Dentel JN, Wiseman RW. Selective inhibition of ATPase
567 activity during contraction alters the activation of p38 MAP kinase isoforms in
568 skeletal muscle. J Cell Biochem. 2013;114(6):1445–55.
569 28. Barclay CJ. The basis of differences in thermodynamic efficiency among skeletal
570 muscles. Clin Exp Pharmacol Physiol. 2017;44(June):1279–86.
571 29. Augusto V, Padovani CR, Eduardo G, Campos R. Skeletal Muscle Fiber Types in
572 C57Bl6J Mice. Braz J Morphol Sci. 2004;21(2):89–94.
573 30. Jennische E. Ischaemia Induced Injury in Glycogen-Depleted Skeletal Muscle.
574 Selective Vulnerability of FG Fibres. Acta Physiol Scandanavia. 1985;125:727–34.
575 31. Law DJ. Myofibrils Bear Most of the Resting Tension in Frog Skeletal Muscle.
576 Science (80-). 1985;230:1280–2.
577 32. Armstrong SC, Latham CA, Shivell CL, Ganote CE. Ischemic Loss of
578 Sarcolemmal Dystrophin and Spectrin: Correlation with Myocardial Injury. J Mol
579 Cell Cardiol. 2001;33(6):1165–79.
580 33. Fielding RA, Manfredi TJ, Ding W, Fiatarone MA, Evans WJ, Cannon JG. Acute
581 phase response in exercise. III. Neutrophil and IL-1 beta accumulation in skeletal
582 muscle. Am Physiol Soc. 1993;265(1):166–72.
583 34. Weibel ER. Exercise-induced maximal metabolic rate scales with muscle aerobic
584 capacity. J Exp Biol. 2005;208(9):1635–44.
585 35. Barclay CJ. Energetics of contraction. Compr Physiol. 2015;5(2):961–95.
586 36. Allen DG, Lamb GD, Westerblad H. Skeletal Muscle Fatigue : Cellular
587 Mechanisms. Physiol Rev. 2008;88:287–332.
588 37. Chin ER, Allen DG. Effects of reduced muscle glycogen concentration on force,
589 Ca2+release and contractile protein function in intact mouse skeletal muscle. J
590 Physiol. 1997;498(1):17–29.

591 38. Ørtenblad N, Westerblad H, Nielsen J. Muscle glycogen stores and fatigue. J
592 Physiol. 2013;591(18):4405–13.
593 39. Adeva-Andany MM, González-Lucán M, Donapetry-García C, Fernández-
594 Fernández C, Ameneiros-Rodríguez E. Glycogen metabolism in humans. BBA
595 Clin. 2016;5:85–100.
596 40. Garber A, Karl I, Kipnis D. Alanine and Glutamine Synthesis and Release from
597 Skeletal Muscle I. J Biol Chem. 1976;251(3):836–43.
598 41. Garber A, Karl I, Kipnis D. Alanine and Glutamine Synthesis and Release from
599 Skeletal Muscle II. J Biol Chem. 1976;251(3):836–43.
600 42. Smith IC, Bombardier E, Vigna C, Tupling AR. ATP Consumption by
601 Sarcoplasmic Reticulum Ca2+ Pumps Accounts for 40-50% of Resting Metabolic
602 Rate in Mouse Fast and Slow Twitch Skeletal Muscle. PLoS One. 2013;8(7):1–11.
603 43. Walker PM. Ischemia/Reperfusion Injury in Skeletal Muscle. Ann Vasc Surg.
604 1991;5(4):399–402.
605 44. Weibel ER, Taylor CR, Weber JM, Vock R, Roberts TJ, Hoppeler H. Design of the
606 oxygen and substrate pathways. VII. Different structural limits for oxygen and
607 substrate supply to muscle mitochondria. J Exp Biol. 1996;199:1699–709.
608 45. Saltin B, Gollnick PD. Skeletal Muscle Adaptability: Significance for Metabolism
609 and Performance. Skelet Muscle. 1983;10:555–631.
610 46. Simoneau J, Bouchard C. Human variation in skeletal muscle fiber-type proportion
611 and enzyme activities. Am J Physiol …. 1989;257(4):567–72.
612 47. Westerblad H, Allen DG, Bruton JD, Andrade FH, Lännergren J. Mechanisms
613 underlying the reduction of isometric force in skeletal muscle fatigue. Acta Physiol
614 Scand. 1998;162(3):253–60.
615 48. Howlett RA, Hogan MC. Effect of hypoxia on fatigue development in rat muscle
616 composed of different fibre types. Exp Physiol. 2007;92(5):887–94.

617 49. Barclay CJ, Constable JK, Gibbs CL. Energetics of fast- and slow- twitch muscles
618 of the mouse. J Physiol. 1993;472:61–80.
619 50. Bonen A, Mcdermott J, Tan M. Glycogenesis and Glyconeogenesis in Skeletal:
620 Effects of pH and Hormones. Am J Physiol - Endocrinol Metab. 1990;258(4):693–
621 700.

622
623
624
625
626
627
628
629
630
631
632
633
634
635
636
637
638
639
640
641
642

643

644

645

646

647
648

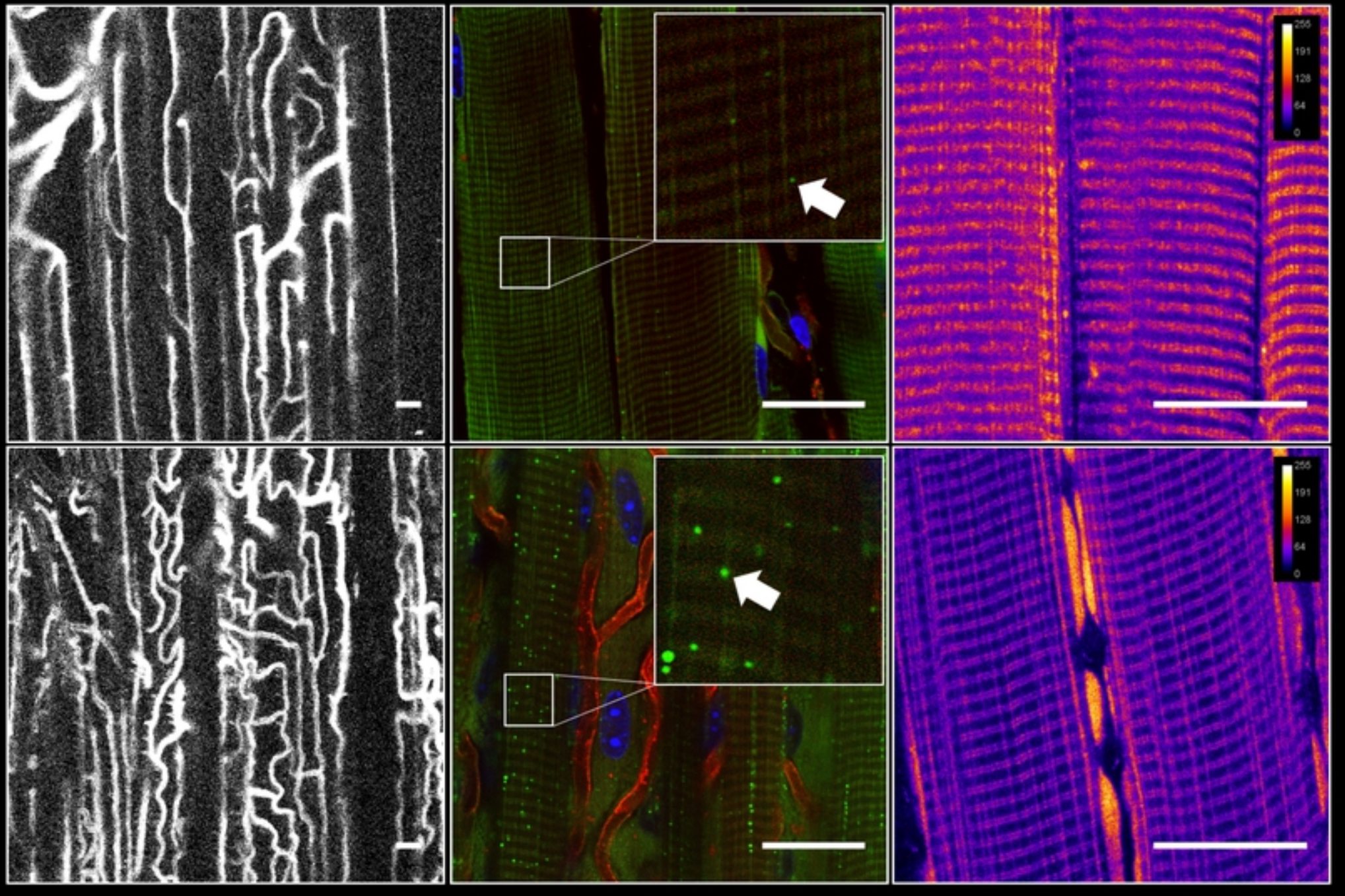

Figure 1

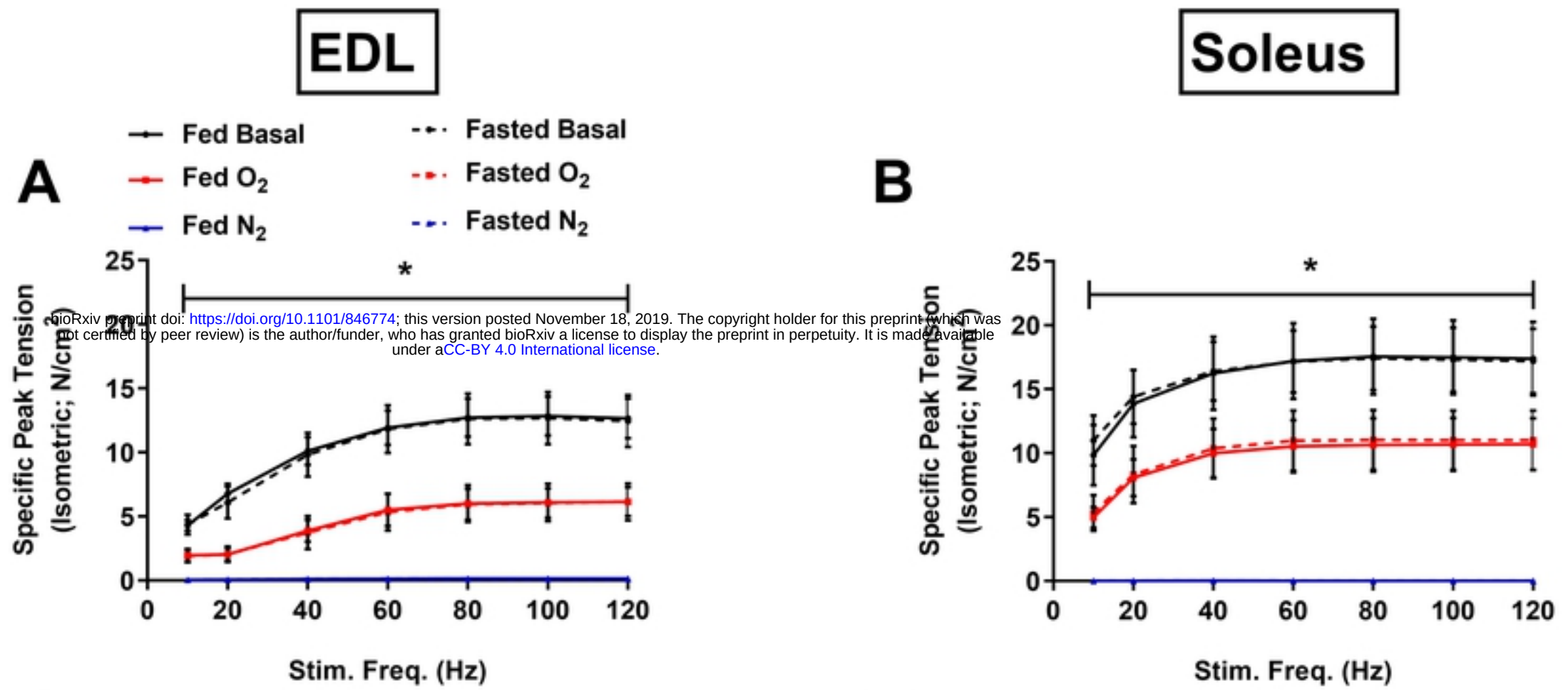

Figure 2

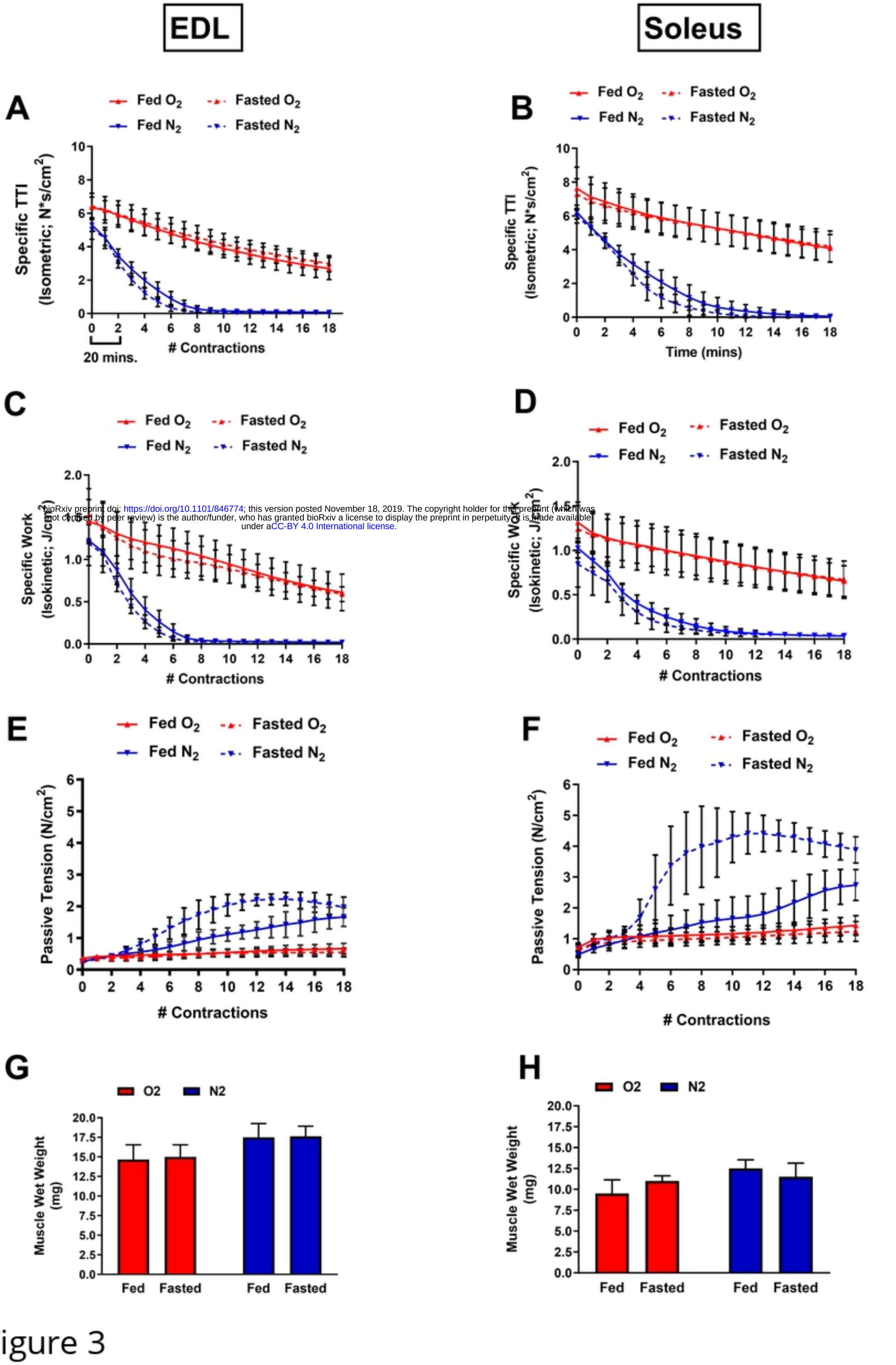

Figure 3

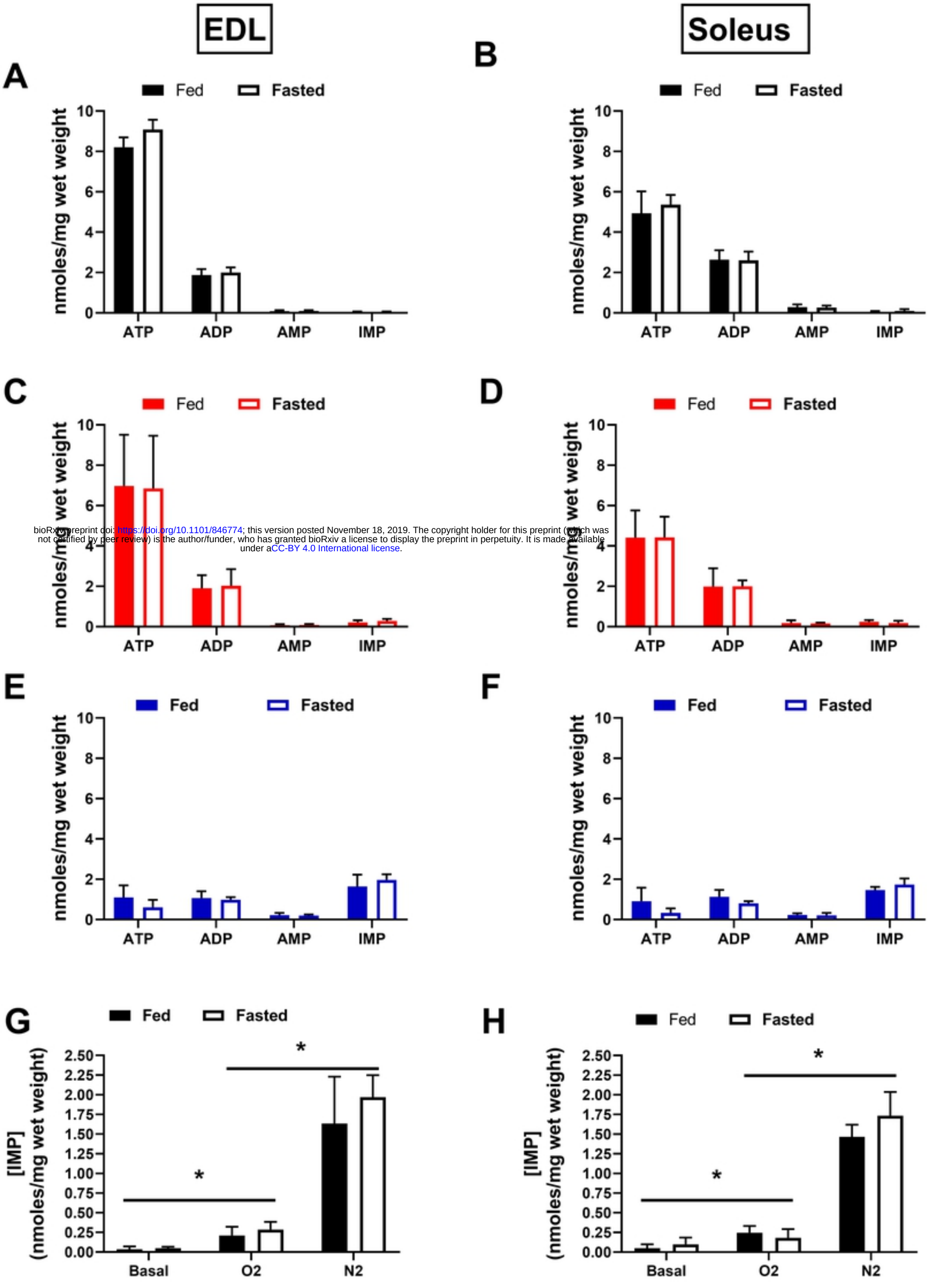

Figure 4

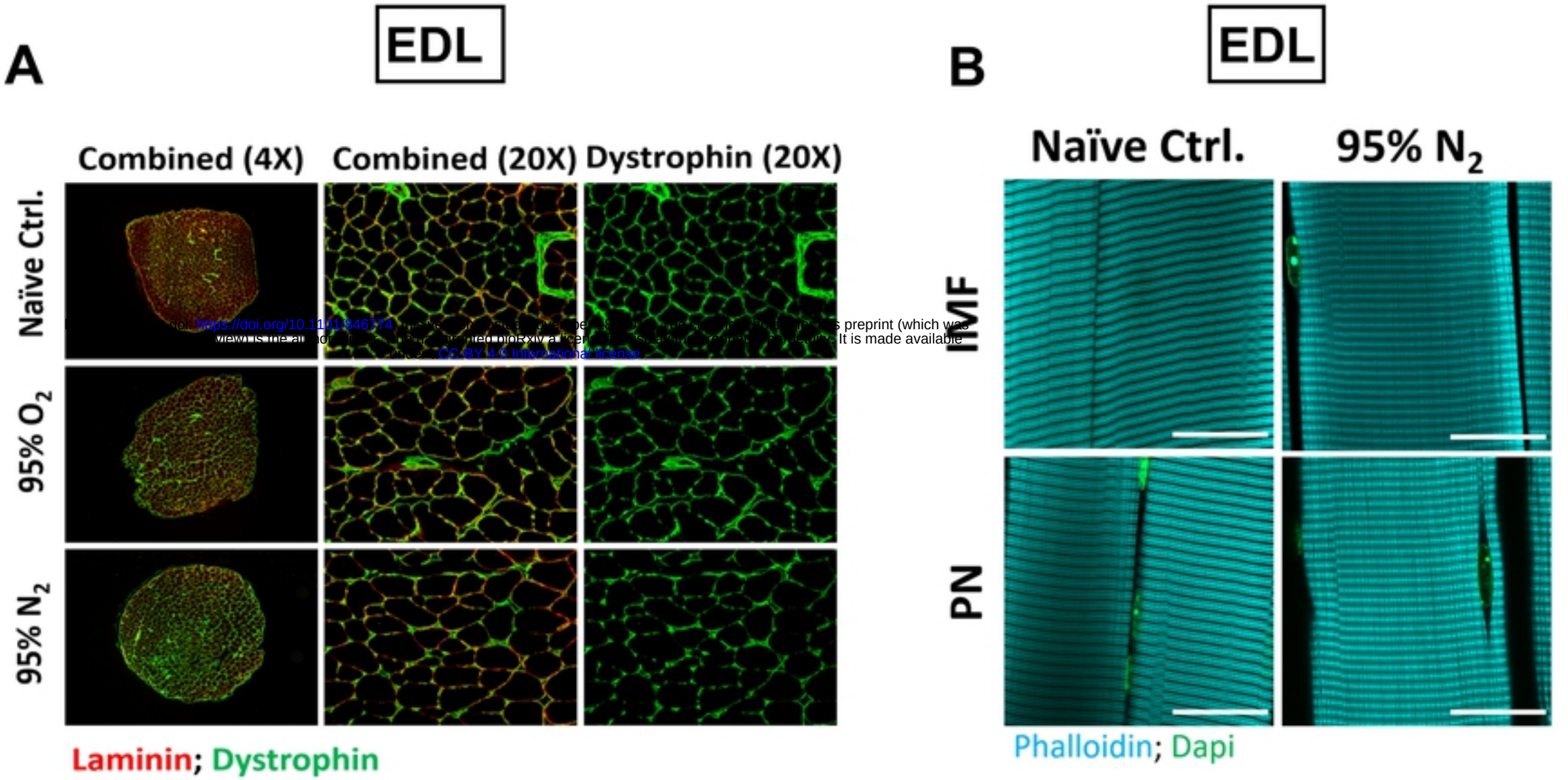

Figure 5